c is small and downstream c remains finite. As mixing takes place in the flow, c is continuous at $x = 0$. The appropriate solution of equation (5) is

$$\begin{aligned} c &= c_0 \exp(Ux/D) \qquad \text{when } x < 0 \\ c &= c_0 \qquad \text{when } x \geqslant 0 \end{aligned} \tag{6}$$

where c_0 depends on the rate of addition of i. For pipe sections downstream from $x = 0$ the mean region residence time of i is V/Q, by the same argument as before. The mean residence time for sections of pipe upstream from the injection point may also be calculated. Indeed the mean residence time in the semi-infinite upstream section is finite: by integration of equation (6) we find that $g_i(0) = c_0 D/U$, while the system transmission rate is Uc_0. Hence

$$\bar{t}_i = D/U^2 \tag{7}$$

As an example of a mean residence time in a stationary medium, consider steady one-dimensional diffusion between a source at $x = L$ and a sink at $x = 0$. The concentration profile is $c = c(L) \cdot x/L$ which gives a steady state holdup (per unit cross-sectional area) of $\frac{1}{2}Lc(L)$. The transmission rate (again per unit c.s.a.) is $\mathscr{D}c(L)/L$, $\mathscr{D}$ being the diffusivity. Applying equation (3), the mean residence time between $x = L$ and $x = 0$ is

$$\bar{t}_i = L^2/2\mathscr{D} \tag{8}$$

The mean residence time for any intermediate section may be found in the same way.

We conclude with an example in which the mean residence time is finite in part of an infinite stationary medium. Substance i is generated in a spherical void, radius r_0, and steadily diffuses away in all directions. The diffusion equation

$$\frac{\mathrm{d}}{\mathrm{d}r}\left(r^2 \frac{\mathrm{d}c}{\mathrm{d}r}\right) = 0 \tag{9}$$

has a solution $c = c_0 r_0/r$ which tends to zero at large distances from the void. Here c_0 is the concentration at r_0. The transmission rate is equal to the rate of diffusion from the void and is $4\pi\mathscr{D}r_0 c_0$. The holdup in the zone $r_0 < r < r_1$, obtained by integration, is $2\pi c_0 r_0 (r_1^2 - r_0^2)$, and thus the mean residence time in this zone is

$$\bar{t}_i = (r_1^2 - r_0^2)/2\mathscr{D} \tag{10}$$

Notice that equation (10) tends to

$$\bar{t}_i = r_1^2/2\mathscr{D} \tag{11}$$

as r_0 tends to zero; now $\bar{t}$ can be thought of as the mean residence time in the neighbourhood of a point source from which material is dispersed by diffusion.

B. A. BUFFHAM

Department of Chemical Engineering,
University of Technology,
Loughborough, Leicester UK

Received 12 June; accepted 23 June 1978.

1. Danckwerts, P. V. *Chem. Engng Sci.* **2**, 1–13 (1953).
2. Grodins, F. S. *Circulation Res.* **10**, 429–446 (1962).
3. Zierler, K. L. *Circulation Res.* **10**, 393–407 (1962).
4. Gibilaro, L. G. *Nature* **270**, 47–48 (1977).
5. Gibilaro, L. G. *Chem. Engng Sci.* **33**, 487–492 (1978).
6. Hearon, J. Z. *Math. Biosci.* **3**, 31–39 (1968).
7. Buffham, B. A. & Kropholler, H. W. *Math. Biosci.* **6**, 179–184 (1970).
8. Buffham, B. A. & Kropholler, H. W. *Chem. Engng Sci.* **28**, 1081–1089 (1973).

α'-Sialon ceramics

OUR previous report[1] on Si–Al–O–N ceramics stated that expanded α-silicon 'nitride' structures had been obtained by reaction of lithium–silicon nitride, $LiSi_2N_3$, with alumina. The unit-cell dimensions of one example (a, 7.822; c, 5.677Å) gave

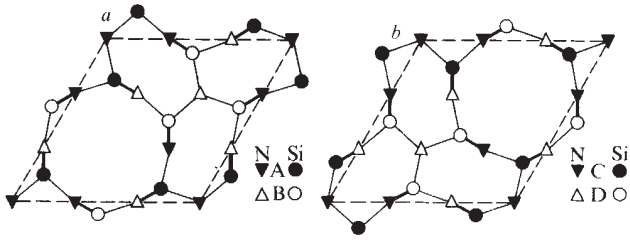

Fig. 1 Idealised Si–N layers in α and β silicon nitrides: *a*, AB layers; *b*, CD Layers. β-structure, ABAB; α structure, ABCD.

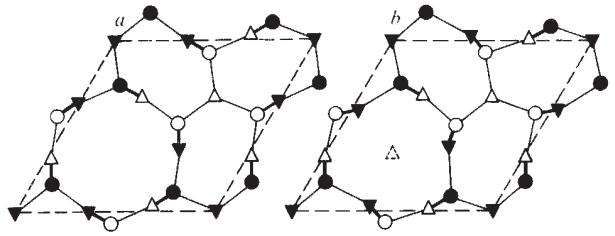

Fig. 2 Actual Si–N layers in α and β silicon nitrides: *a*, in β; *b*, in α.

a cell volume about 3% greater than that of α-silicon nitride. Subsequent work[2] showed a variation in dimensions for the α'-lithium sialon when lithium aluminate, $LiAlO_2$, was reacted in different proportions with Si_3N_4. However, other phases, such as β'-sialon and nitrogen–eucryptite, were always present and the product never contained more than ~30% of the α' material. $\alpha\upsilon$-Sialons were also found in the Mg–Si–Al–O–N system[3] but again never pure, and were observed by Masaki *et al.*[4] during the nitriding of silicon with AlN and Al_2O_3 additions. A recent claim by Mitomo[5] of α' solid solutions of Si_3N_4–Al_2O_3 and/or Si_3N_4–Y_2O_3 occurring during the sintering of Si_3N_4 at 1,700–1,800 °C with Al_2O_3–Y_2O_3 mixtures prompted this report of the preparation and characterisation of pure α'-phases in M–Si–Al–O–N systems where M is Li, Ca or Y. Such phases also occur, but have not so far been prepared in a pure form, in magnesium and other sialon systems.

The 'idealised' silicon nitride structure can be described as a stacking of Si–N layers in either an ABAB... (β) or an ABCD... (α) sequence as shown in Fig. 1. This gives long continuous channels in β, parallel to the hexagonal c-direction and centred at 2/3, 1/3 in the outlined cell of Fig. 1*a*. In α, the c-glide plane relating the layers CD with AB replaces the continuous channels of the β structure by large closed interstices at 1/3, 2/3, 3/8 and 2/3, 1/3, 7/8. In the α unit cell containing, ideally, $Si_{12}N_{16}$ there are therefore two sites large enough to accommodate other atoms or ions. Although the Si–N layers in the actual β structure are almost identical with the 'ideal' configurations (see Fig. 2), those of α are considerably distorted and nitrogen atoms at heights approximately 3/8 and 7/8 are shifted towards the centres of the two respective interstices.

All the α'-sialons have compositions represented by $M_x(Si, Al)_{12}(O, N)_{16}$ where $x \not> 2$. Cell dimensions of examples where $x \not> 1$, are compared with those of α and β silicon nitrides in Table 1. There are small but distinct differences between the X-ray diffracted intensities of α and α' and a complete structure determination for a composition near $Ca[Si_9Al_3ON_{15}]$ shows that each of the two interstitial sites contains on average half a Ca atom.

The α'-structure is derived from α-$Si_{12}N_{16}$ by partial replacement of Si with Al. Valency compensation is effected by the 'modifying' cations (Li, Ca, Y) occupying the interstices of the (Si, Al)–N 'network' but where a modifier oxide is used, oxygen may also replace nitrogen. When α' is synthesised entirely from nitrides, for example, a mixture of Si_3N_4, AlN and Ca_3N_2, the product contains no oxygen, and valency

0028–0836/78/0274—0880$01.00

Table 1 Unit-cell dimensions and densities of α'-sialons and α and β silicon nitrides

	a	c	c/a	d_o	d_c
β-Si_3N_4	7.61	2.91	0.765/2	3.192	3.192
α-Si_3N_4	7.76	5.62	0.724	3.16*	3.183
$LiSi_{10}Al_2ON_{15}$	7.83	5.67	0.724	3.12	3.14
$Ca_{0.5}Si_{10.5}Al_{1.5}O_{0.5}N_{15.5}$	7.82	5.68	0.727	3.16	3.20
$Ca_{0.8}Si_{9.2}Al_{2.8}O_{1.2}N_{14.8}$	7.86	5.71	0.727	3.19	3.26
$Y_{0.4}Si_{10}Al_2O_{0.8}N_{15.2}$	7.81	5.69	0.729	3.23	3.25
$Y_{0.6}Si_{9.2}Al_{2.8}O_{1.1}N_{14.9}$	7.83	5.71	0.729	3.28	3.36

d_o, observed density; d_c, calculated density;
* Range of values 3.167–3.171 g ml^{-1} obtained by Wild *et al.* for α-needles produced by SiO–N_2 reaction[6].

compensation is due solely to the introduction of modifying cations. Because there are only two sites per unit cell for these, the limiting composition for Ca-α'-nitride is $Ca_2Si_8Al_4N_{16}$. The limit for the corresponding oxynitride is also two calciums per unit cell but the extent of the replacement of silicon by aluminium and oxygen by nitrogen has not yet been determined.

The α'-sialons are prepared by heating appropriate mixtures of nitrides or nitrides plus oxides at 1,750 °C in one atmosphere of molecular nitrogen or argon for 15 min. Weight losses are neglible and the composition of the initial mix, calculated from the proportions of powder constituents with allowance for surface oxide on the nitrides, is virtually identical with direct microanalysis of the product using a Camebax electron probe at AERE, Harwell. Moreover, densities calculated from compositions, cell dimensions and the proposed structures are, as shown in Table 1, in excellent agreement with the observed densities.

Typical X-ray photographs of Ca, Li and Y α'-sialons are shown in Fig. 3 from which it is clear that exactly the same product is obtained starting with β-Si_3N_4 as with α-Si_3N_4. Unlike the β'-sialons, $Si_{6-z}Al_zO_zN_{8-z}$, where the replacement without structural change is (Si–N) by (Al–O), the replacement in α'-phases is largely (Si–N) by (Al–N). With bond lengths Si–N ~ 1.74, Al–O ~ 1.75 and Al–N ~ 1.87 Å, the relative increases in unit-cell dimensions for $\alpha \rightarrow \alpha'$ are much greater than for $\beta \rightarrow \beta'$. For a general composition

$$M_xSi_{12-(m+n)}Al_{(m+n)}O_nN_{16-n}$$

there are m(Si–N) replaced by m(Al–N) replaced by n(Al–O). If the unit-cell dimensional changes corresponding to these respective replacements are in the ratio 5 : 1, Fig. 4 shows that the observed dimensions for a range of α'-phases fit the relationships:

$$\Delta a\ (\text{Å}) = 0.045m + 0.009n \quad (1)$$

$$\Delta c\ (\text{Å}) = 0.04m + 0.008n \quad (2)$$

The X-ray photographs of Fig. 5 show that α' reacts with Al_2O_3 to give β' and β' reacts with AlN plus the appropriate modifier nitride (such as Ca_3N_2) to give α'. Equations corresponding to these reactions are:

$$\underbrace{Y_{0.4}Si_{9.4}Al_{2.6}O_{1.3}N_{14.7}}_{\alpha'} + (2.7)Al_2O_3$$

$$\xrightarrow{1750°C} \underbrace{(2.85)Si_{3.16}Al_{2.84}O_{2.84}O_{2.84}N_{5.16}}_{\beta',\ z=2.84} + (0.2)Y_2Si_2O_7 \quad (3)$$

$$\underbrace{(1.45)Si_{4.85}Al_{1.15}O_{1.15}N_{6.85}}_{\beta',\ z=1.15} + (0.56)Ca_3N_2 + (3.34)AlN$$

$$\xrightarrow{1,750°C} \underbrace{Ca_{1.17}Si_{7.0}Al_{5.0}O_{1.7}N_{14.3}}_{\alpha'} \quad (4)$$

Just as β'-sialons can be produced by nitriding mixtures of oxides and carbon with molecular nitrogen, so also can these

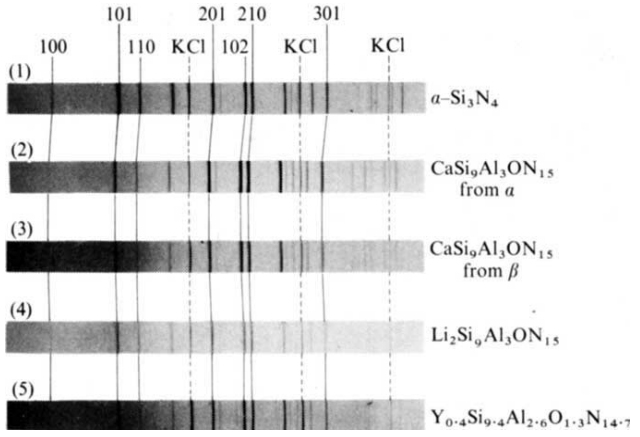

Fig. 3 Typical X-ray powder patterns of Ca, Li and Y α'-sialons. CuKα radiation; Hägg–Guinier focusing camera.

α'-phases. Calcium compounds have been prepared in this way at temperatures as low as 1,400 °C. Technological advantages of α' compared with β' sialons are not yet known but it seems that the field for exploration has been considerably widened.

The α' compositions so far observed that are closest to Si_3N_4 are

$$Ca_{0.5}Si_{10.5}Al_{1.5}O_{0.5}N_{15.5} \quad (5)$$

and

$$Y_{0.3}Si_{10.5}Al_{1.5}O_{0.5}N_{15.5} \quad (6)$$

If it is accepted that α' requires the equivalent of at least half a cationic valency ($Ca_{0.25}$ or $Y_{0.16}$) in each of the two interstices to stabilise the structure, it is suggested that this is also the requirement in 'pure' α-silicon nitride. The corresponding compositions are then

$$Si^{3+}_{0.3}Si^{4+}_{11.8}N^{3-}_{16} \quad (7)$$

and

$$Si^{3+}_{0.3}Si^{4+}_{11.6}O^{2-}_{0.5}N^{3-}_{15.5} \quad (8)$$

depending on whether oxygen is available for valency compensation. It is assumed that only Si^{3+}, and not Si^{4+}, is large enough to be accommodated in the structural interstices; the observed lengths of 2.2 Å for these Si–N bonds seem reasonable. Certainly, there seems no reason for the structural distortion of α and α' other than partial occupation of such sites. It is hardly fortuitous that the calculated density for the α composition, equation (8), 3.170 g ml^{-1}, almost exactly agrees with the density range observed[6] for α needles produced by reaction of silicon monoxide with nitrogen, 3.167–3.171 g ml^{-1}, and which cannot be explained by the composition Si_3N_4. The unit-cell dimensions determined by one of us (D.P.T.) for 26 different α-silicon nitrides prepared by (1) reacting Si with N_2; (2) the reaction of SiO with N_2; and (3) chemical vapour deposition from silicon halides, vary widely within limits $a = 7.7491$–7.7619 and $c = 5.6151$–5.6221 Å.

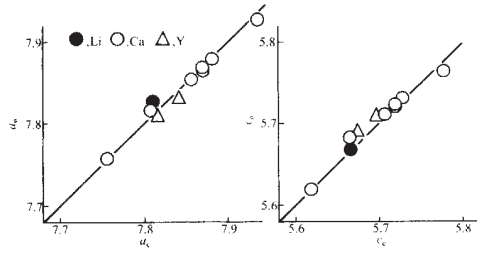

Fig. 4 Observed (o) and calculated (c) unit-cell dimensions for α'-sialons $M_xSi_{12-(m+n)}Al_{(m+n)}O_nN_{16-n}$; $m = 1$–4; $n = 0$–2.5. $\Delta a_c = 0.045m + 0.009n$ Å; $\Delta c_c = 0.04m + 0.008n$ Å. Si–N, 1.74 Å; Al–N, 1.87 Å; Al–O, 1.75 Å.

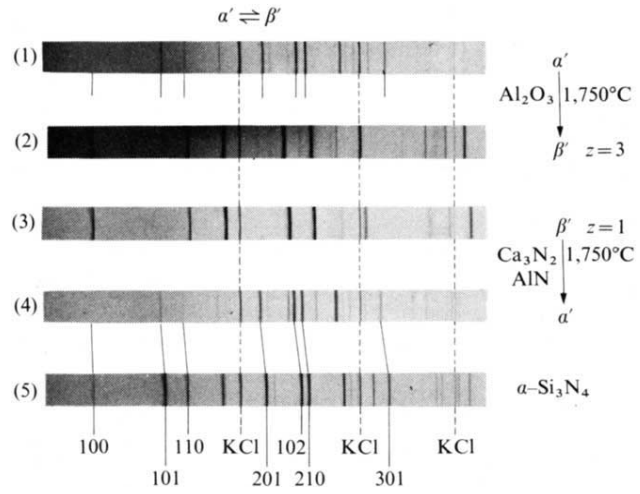

Fig. 5 X-ray powder patterns showing transformations $\alpha' \rightleftharpoons \beta'$ CuKα radiation; Hägg–Guinier focusing camera.

Considering that the same precise method was used in each case by the same investigator, this variation is well outside any experimental error (±0.0005 Å) and is thought to be due to variation within the range of compositions given by equations (7) and (8). It is further suggested that the transformations $\alpha \rightleftharpoons \beta$ and $\alpha' \rightleftharpoons \beta'$ take place only by liquid-phase or vapour-phase processes. Further details will be published elsewhere.

S. HAMPSHIRE
H. K. PARK
D. P. THOMPSON
K. H. JACK

Wolfson Research Group for High-Strength Materials, Crystallography Laboratory, The University, Newcastle upon Tyne, UK

Received 8 May; accepted 15 June 1978.

1. Jack, K. H. & Wilson, W. I. *Nature phys. Sci.* **238,** 28 (1972).
2. Jama, S. A. B., Thompson, D. P. & Jack, K. H. *Special Ceramics* **6** (ed. Popper, P.) 299 (BCRA, Stoke-on-Trent, 1975).
3. Jack, K. H. *J. materials Sci.* **11,** 1135 (1976).
4. Masaki, H., Oyama, Y. & Kamigaito, O. *Jap. J. appl. Phys.* **14,** 301 (1975).
5. Mitomo, M. *Yogyo-Kyokai-Shi* **85,** 50 (1977).
6. Wild, S., Grieveson, P. & Jack, K. H. *Special Ceramics* **5** (ed. Popper, P.) 385 (BCRA, Stoke-on-Trent, 1972).

The Rankine–Hugoniot relation for shock waves in very porous media

AN entropy rise accompanies shock wave propagation in any medium. The entropy jump at a shock front is especially high when a medium contains a large number of pores—small empty holes randomly distributed. Shock compression of a porous medium leads to intense heating of the material surrounding the pores because of its nonelastic deformation. Intense heating of a porous material at a shock front yields an 'anomalous' shape for the Rankine–Hugoniot curve on the p–V plane[1,2]. This effect of porosity was clearly seen in our experiments with cast foamed polystyrene of various initial densities, ρ_0. The solid lines in Fig. 1 represent Rankine–Hugoniot curves obtained experimentally. It can be seen that the specific volume of compressed material is much greater than the volume of polystyrene in the condensed (solid or liquid) state. It is clear that such a great increase in volume is possible only when initially condensed porous material turns into the gaseous state, and cannot be explained in terms of thermal expansion.

Photographs by high speed camera (Fig. 2) confirm that shock-wave compression of very porous polystyrene is associated with a transition into the gaseous phase. Figure 2 shows that propagation of a shock wave in porous polystyrene (the arrow in Fig. 1 indicates the corresponding p–V values) is followed by a very intense expansion flow of compressed material. The expansion flow must be related to the gasification of polystyrene, because it was found experimentally that a decrease of air pressure in the pores to 5×10^{-5} atm had no effect on rarefaction.

The overall pattern of a shock front followed by intense expansion flow of gasified material shows more similarities to a detonation wave than to a shock wave in a homogeneous medium. Experimental data must therefore be explained by analogy with a detonation wave. Thus to correct the Rankine–Hugoniot relation for the case considered we must take into account a phase state transition taking place at a shock front which is (in contrast to detonation) endothermic.

If w, p and V are enthalpy, pressure and specific volume respectively and subscripts o and s denote the states of the material in front of and behind a shock wave, the Rankine–Hugoniot relation may be written in the form

$$w_s - w_o + \lambda_v = \tfrac{1}{2}(p_s - p_o)(V_s + V_o)$$

where λ_v is the heat of gasification (vaporisation, sublimation, chemical decomposition and so on). In general, p_o and w_o are small in comparison with the other terms of the equation and one may put $p_o = 0$, $w_o = 0$. Enthalpy w_s can be expressed by one of the equations of state for dense real gases. For a gas at moderate density,

$$pV = RT\left(1 + \frac{b}{V}\right)$$

which gives for w_s

$$w_s = c_p T = \left(\gamma \frac{P_s V_s}{\gamma - 1}\right) \Big/ \left(1 + \frac{b}{V}\right)$$

(R is the gas constant; T, temperature; b, second Van-der-Waals constant; $\gamma = c_p/c_v$; 'Poisson's ratio'). Substituting w_s in

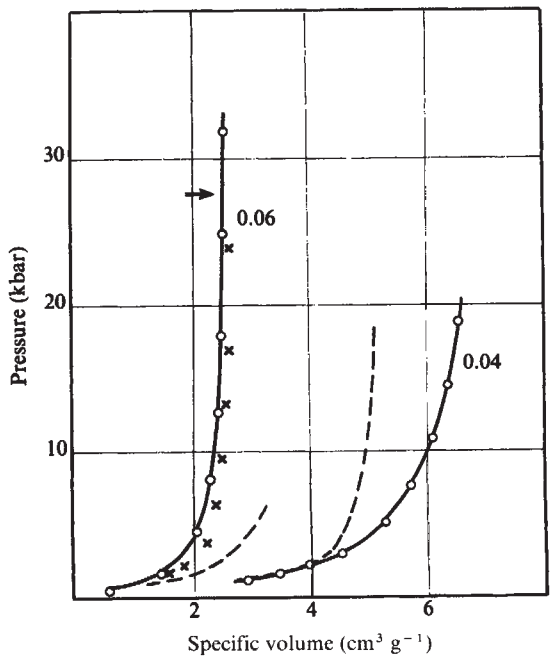

Fig. 1 Experimental (solid lines) and computed (broken lines and crosses) Rankine–Hugoniot curves for cast foamed polystyrene of low density. Values shown against lines are initial densities in g cm^{-3} (ref. 2).

0028–0836/78/0274—0882$01.00